Applied Bionics and Biomechanics 10 (2013) 159–173
DOI 10.3233/ABB-140083
IOS Press

Measurement and quantification of gross human shoulder motion

Jeremy T. Newkirk[a,*], Martin Tomšič[b], Charles R. Crowell[c], Michael A. Villano[c] and Michael M. Stanišić[d]
[a]*Mechatronics Corporate Research Center, ABB Inc, Windsor, CT, USA*
[b]*Automation, Cybernetics and Robotics, Jozef Stefan Institute, Ljubljana, Slovenia*
[c]*Department of Psychology, University of Notre Dame, Notre Dame, IN, USA*
[d]*Aerospace and Mechanical Engineering Department, University of Notre Dame, Notre Dame, IN, USA*

Abstract. The shoulder girdle plays an important role in the large pointing workspace that humans enjoy. The goal of this work was to characterize the human shoulder girdle motion in relation to the arm. The overall motion of the human shoulder girdle was characterized based on motion studies completed on test subjects during voluntary (natural/unforced) motion. The collected data from the experiments were used to develop surface fit equations that represent the position and orientation of the glenohumeral joint for a given humeral pointing direction. These equations completely quantify gross human shoulder girdle motion relative to the humerus. The equations are presented along with goodness-of-fit results that indicate the equations well approximate the motion of the human glenohumeral joint. This is the first time the motion has been quantified for the entire workspace, and the equations provide a reference against which to compare future work.

Keywords: Shoulder girdle, motion studies, shoulder motion

1. Introduction

In this work the motion of the human shoulder was studied relative to the motion of the upper arm, referred to as the humerus throughout this paper. The human shoulder is a complex mechanism made up of two parts that move together in a coordinated fashion [25, 30]. The outermost part, made up of the anterior of the humerus connected to the scapula via the glenohumeral joint, is generally considered to be the shoulder. The glenohumeral joint is approximated to be a ball-and-socket joint. The inner part, referred to as the "shoulder girdle", is often neglected due to its complexity, but it plays a critical role in the motion of the shoulder [21]. The motion of the shoulder girdle is the major focus of this work because its contribution significally increases the pointing workspace of the shoulder. Definitions for the terminology describing position, motion and anatomical planes throughout this paper can be found in [23, 25, 30].

The human shoulder girdle, shown in Fig. 1, is a closed-loop (parallel) mechanism made up of the sternum, clavicle and scapula. A thorough description of the shoulder girdle can be found in [25]. The human mechanism begins medially at the sternum of the thorax, which is connected by the sternoclavicular joint to the clavicle. Moving laterally, the clavicle is connected by the acromioclavicular joint to the acromion of the scapula. The scapula is then connected to the posterior of the thorax via the scapulothoracic

*Corresponding author: Jeremy T. Newkirk, Mechatronics Corporate Research Center, ABB Inc, Windsor, CT 06095, USA. Tel.: +574 309 2433; E-mail: jnewkirk@alumni.nd.edu.

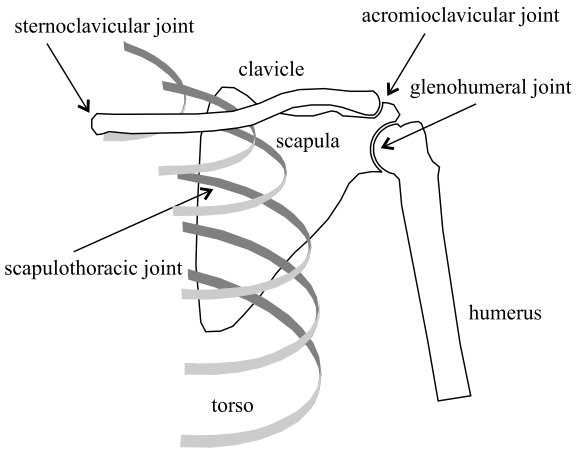

Fig. 1. The Human Shoulder Girdle [20].

joint, which completes the circuit. The sternoclavicular and acromioclavicular joints are synovial, meaning they are encapsulated and surrounded by a lubricating fluid. Synovial joints are the most common joint type found in the human body. The scapulothoracic joint is a unique and very complex joint that is the only non-synovial joint found in the human body. In the scapulothoracic joint, the scapula "glides" over and between muscles on the posterior of the thorax. Typical of parallel mechanisms, the workspace of the scapula is relatively small, but the rigidity of the parallel mechanism provides good support for the serial arm that connects to the parallel mechanism at the glenohumeral joint on the scapula.

In [20], the human shoulder girdle is shown to be approximately a 2-degree-of-freedom (DOF) system. This is shown by using the Chebychev–Grüebler–Kützbach criterion

$$F = 6(\underbrace{N}_{2}) - 3(\underbrace{p_3}_{3}) = 12 - 9 = 3, \quad (1)$$

where N represents the number of moving links (clavicle and scapula in this case) and p_3 is the number of joints that remove 3-DOF, which are the spherical joint approximations of the sternoclavicular and acromioclavicular joints and the planar approximation of the scapulothoracic joint. The spherical joint approximations on either end of the clavicle allow it to spin around an axis passing through the two joint centers, which does not contribute to the overal motion of the mechanism. Therefore, the mechanism has 2 actual DOF. The human shoulder has ligaments, tendons and muscle that prevent the clavicle from rotating freely.

The primary function of the shoulder girdle is to provide stability for and increase the mobility of the glenohumeral joint [10]. It points the central axis of the glenoid fossa (the socket of the glenohumeral joint on the scapula) in a coupled fashion with articulation of the humerus. This is often called the "shoulder rhythm" or "scapulohumeral rhythm" [30]. This scapulohumeral rhythm significantly increases the pointing workspace of the humerus by acting as a double pointing mechanism [26]. As the humerus rotates about a particular axis, the shoulder girdle rotates the scapula in approximately the same direction about a similar axis. This is significant because the contribution of the glenohumeral joint to humeral pointing is limited to approximately 120° of angular displacement [15]. However, the maximum angular displacement of the humerus relative to a thorax fixed frame (referred to as 'sternum' throughout this dissertation for simplicity) has been shown to be approximately 180° [3, 6, 8, 12, 14, 16, 17]. The motion of the shoulder girdle makes up the difference in angular displacement, increasing the pointing workspace of the humerus up to 50%.

Another aspect of the shoulder girdle is that it moves the location of the glenoid fossa relative to the sternum. As the pointing direction of the central axis of the glenoid fossa is altered, the location moves as well. This causes a shortening or lengthening of the distance from the sternum to the glenoid fossa, which is referred to here as "shoulder heaving". As with the scapulohumeral rhythm, shoulder heaving is also coupled to

articulation of the humerus. When the humerus performs abduction and adduction in the transverse plane, there is an elongation and contraction of the distance from the sternum to the glenoid fossa, respectively. Lateral abduction of the humerus in the frontal plane causes this distance to contract. When the humerus performs flexion and extension in the saggital plane, the distance maintains a constant length. Shoulder heaving has not been well understood or quantified. In [18], shoulder heaving is described for humeral abduction and adduction, but it has not been quantified for other types of humerus motion. The motion of the glenoid fossa is an important function of the shoulder girdle as it allows for humans to accomplish movements that would otherwise not be possible. For example, as the humerus is rotated forward, the location of the glenoid fossa is also moved forward, which allows the humerus to be pointed across the chest.

2. Motion studies

Human shoulder motion studies were conducted to characterize the motion of the shoulder girdle relative to humeral pointing. This characterization is important to better understand how the shoulder girdle contributes to the large pointing workspace that humans enjoy. This work quantifies scapular rotation as well as shoulder heaving relative to humeral motion in a general sense. The humeral motion was not constrained to a plane, but rather the overall workspace of the humerus was considered. The human shoulder motion studies described here look at the entire range of motion of the humerus, allowing each subject to move his or her humerus throughout its entire workspace in a voluntary fashion (i.e. unforced/natural motion). A large pool of subjects was used to derive general relationships between the motion within the shoulder girdle and humeral motion. This enabled assessment of the variability across subjects and ensured that the relationships were not largely influenced by a few outlier subjects. The motions were recorded dynamically, so the translations and rotations were captured during normal motion of the arm and shoulder.

The first set of motion studies were completed using an electromagnetic motion capture system called "Flock of Birds" [2]. These motion studies were conducted in the Psychology department at the University of Notre Dame. This set of studies included 20 subjects, 10 male and 10 female, selected among volunteers from the graduate students in the Aerospace and Mechanical Engineering department. The average age of the subjects was 25.3 ± 1.4 (mean $\pm$ st. dev.) years. The female subject heights ranged from 150 to 175 cm, with an average of 165.8 ± 6.8 cm. The male subject heights ranged from 168 to 185 cm, with an average of 178.9 ± 6.2 cm. The average height for all subjects was 172.4 ± 9.2 cm. All of the studies were conducted on the right shoulder, and most subjects were right-handed, as only one male and one female were left-handed. The subjects selected reported no prior injuries that would limit or otherwise affect their shoulder motion. Informed consent was obtained from all subjects, and approval was received from the university's Intstitutional Review Board (IRB) before the studies were conducted.

The "Flock of Birds" system uses wired electromagnetic sensors that send their x-y-z location relative to a transmitter back to a receiver. The positional resolution of the sensors is 0.03" (0.08 cm) at 12" (31 cm) from the transmitter, and the sampling rate for the system is 100 Hz. The system was located on a wooden stage, which kept it away from the walls and floor to minimize the interference from metal objects therein. A wooden chair was placed on the stage in which the subjects sat while the motion studies were conducted. The chair was placed such that the x-axis ran from left to right (medial to lateral for the right shoulder), the y-axis from back to front (posterior to anterior) and the z-axis vertically upwards (superior direction). This coordinate system follows the same convention used in [18]. The subjects were fitted with a compression shirt, which had 9 sensors sewn to it. The idea was that the compression shirt would stretch as the subject moved, allowing the sensors to follow the path of the shoulder movement. The 9 sensors were arranged as shown in Fig. 2: 2 on the front of the shirt aligned vertically in line with the sternum, 1 in line with the cervical spine near the last vertebrae, 3 evenly spaced surrounding the glenohumeral joint and 3 evenly spaced surrounding the elbow joint. Sensors 1, 2, 3 and 5 were placed according to the recommendations of the International Society of Biomechanics (ISB) [29]. The recommendations are also supported by the International Shoulder Group (ISG). Sensor 2 represented the origin of the reference frame for this work. Sensors 4 and 6 were placed strategically in an effort to capture gross motion of the shoulder girdle, not just the individual bones (clavicle, scapula and humerus) contained within. The protocol set forth by

Fig. 2. Sensor placement.

the ISB was only designed to capture motion of the bones, and relies on methods such as regression analysis [24] or calculating the pivot point of instantaneous helical axes [27, 28] to locate the glenohumeral joint. For this work, the center of the glenohumeral joint is located by taking the average position of the three sensors that surround it (4, 5 and 6). These sensors also define a plane, so the pointing direction of the central axis of the glenohumeral joint could then be calculated as the unit vector normal to this plane. The logic behind the placement of sensors 7, 8 and 9 was to provide the location of the center of the end of the humerus at the elbow joint. The placements differ from the recommendations of the ISB because that protocol seeks to enable location of the elbow axis. For this work, the subjects were asked to keep their arms straight, i.e. no elbow flexion, throughout the motion studies, as information about the elbow axis was not relevant.

The subjects were asked to move their arms through what each felt was his or her entire range of motion in a voluntary fashion. Each subject was asked to perform this motion for 30 seconds while data were collected. This was completed for all 20 subjects.

The second set of motion studies were conducted using an optical motion capture system from Northern Digital Inc. called "NDI 3D Investigator Motion Capture System". This work was completed in the Automation, Biocybernetics and Robotics lab at the Jožef Stefan Institute. This set of studies included 17 subjects, 11 male and 6 female, selected among volunteers from the researchers working in the lab. The average age was 27.6 ± 3.2 years. The female subject heights ranged from 163 to 178 cm, with an average of 169.0 ± 6.4 cm. The male subject heights ranged from 173 to 185 cm, with an average of 179.8 ± 4.6 cm. The average height for all subjects was 176.0 ± 7.4 cm. All of the subjects in this study were right-handed. The subjects reported no prior injuries that would limit or otherwise affect their shoulder motion. Informed consent was obtained from all subjects prior to conducting human motion studies.

This system uses two cameras and active infrared markers, where the cameras track the x-y-z locations of the markers and send this information back to a receiver. The positional resolution of the sensors is 0.1 cm, and the maximum sampling rate for the system is $4600/(n + 1.3)$ Hz, where n refers to the number of markers used. The sampling rate was selected to be 100 Hz to coincide with the samping rate from the first set of studies. The reference frame, origin and sensor locations were the same as in the first set of motion studies. For this equipment, there was no need for a wooden stage, so the chair was placed on the floor in the same orientation as before. The subjects were fitted with sensors in the same fashion as previously; however, for this study they were attached to

the subjects using double-sided tape. The subjects were asked to wear a tank top so the sensors could be placed directly on the skin. In these motion studies the subjects were asked to move their arms through their entire workspaces in a voluntary fashion while keeping their arms straight for 60 seconds. This was repeated for all 17 subjects.

Only healthy, young adults were selected for the motion studies. This means that the results may not accurately reflect the motion of an injured shoulder or the motion found in the shoulders of children or older adults.

3. Data analysis

The analyses of the collected data are descibed in this section. The first step was to convert the x-y-z locations of the sensors into vectors originating at the sternum. The uppermost sensor on the front of the shirt was defined as the location of the sternum and the origin for this work. The locations of the other sensors were used to determine the humeral pointing direction, the x-y-z locations of the glenohumeral joint relative to the sternum (average of the three shoulder sensors) and the pointing direction of the unit vector normal to the plane created by the three shoulder sensors (referred to throughout this dissertation as the glenoid fossa pointing direction for simplicity). For the humeral pointing direction, a normalized vector $\hat{x}_h$ from the centroid of the three shoulder sensors to the centroid of the three elbow sensors was created,

$$\hat{x}_h = \frac{\mathbf{x}_{el} - \mathbf{x}_{sh}}{\|\mathbf{x}_{el} - \mathbf{x}_{sh}\|}, \tag{2}$$

where $\mathbf{x}_{el}$ is the centroid of the 3 elbow sensors and $\mathbf{x}_{sh}$ is the centroid of the 3 shoulder sensors. The humeral pointing direction angles were calculated by determining the spherical coordinate angles of rotation, azimuth (az) and elevation (el) from the positive x-axis. This is shown graphically in Fig. 3 and the equations are

$$\begin{aligned} \psi &= \text{atan2}\left(\frac{y_h}{x_h}\right) \\ \rho &= \text{asin}(z_h), \end{aligned} \tag{3}$$

where ψ is the az angle and ρ is the el angle and both have units of degrees for this work. The variables x_h, y_h and z_h are the vector components of $\hat{x}_h$ and are unitless. The computer function atan2 is used to determine the atan of a quantity while keeping track of sign information, so the solution corresponding to the proper quadrant is found. A unit vector $\hat{x}$ normal to the plane created by the three shoulder sensors was created to determine the pointing direction of the central axis of the glenoid fossa. This was accomplished via definition that the dot product of two orthogonal vectors is zero. The unit vector was calculated by creating two vectors from the location of one sensor to the other two, and setting the dot product of each vector with $\hat{x}$ equal to zero,

$$\mathbf{x}_i \cdot \hat{x} = \mathbf{0}, \qquad i = 1, 2, \tag{4}$$

where $\mathbf{x}_1$ is a vector from the location of sensor 4 to the location of sensor 5, $\mathbf{x}_2$ is a vector from the location of sensor 4 to the location of sensor 6 in Fig. 2 and $\mathbf{0}$ is the vector representation of zero. Because $\hat{x}$ is a unit vector, it also has the constraint

$$\|\hat{x}\| = 1. \tag{5}$$

This provides 3 equations, 2 from (4) and 1 from (5), with 3 unknowns. Solving this system of equations for the components of $\hat{x}$, $\{x_\zeta, y_\zeta, z_\zeta\}$, leads to two solution sets,

$$\begin{aligned} x_\zeta &= \frac{\mp y_2 z_1 \pm y_1 z_2}{\sqrt{x_2^2(y_1^2 + z_1^2) + (y_2 z_1 - y_1 z_2)^2 - 2x_1 x_2(y_1 y_2 + z_1 z_2) + x_1^2(y_2^2 + z_2^2)}}, \\ y_\zeta &= \frac{\pm x_2 z_1 \mp x_1 z_2}{\sqrt{x_2^2(y_1^2 + z_1^2) + (y_2 z_1 - y_1 z_2)^2 - 2x_1 x_2(y_1 y_2 + z_1 z_2) + x_1^2(y_2^2 + z_2^2)}}, \\ z_\zeta &= \frac{\mp x_2 y_1 \pm x_1 y_2}{\sqrt{x_2^2(y_1^2 + z_1^2) + (y_2 z_1 - y_1 z_2)^2 - 2x_1 x_2(y_1 y_2 + z_1 z_2) + x_1^2(y_2^2 + z_2^2)}}, \end{aligned} \tag{6}$$

where x_1, y_1 and z_1 are the vector components of $\mathbf{x}_1$ and x_2, y_2 and z_2 are the vector components of $\mathbf{x}_2$. The top line of symbols $\pm$ and $\mp$ correspond to a positive

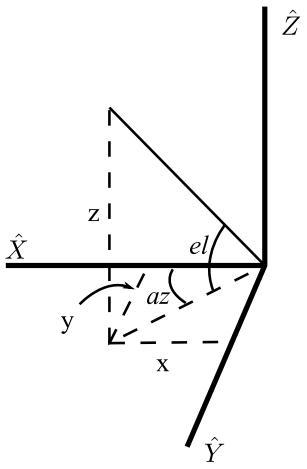

Fig. 3. Geometric representation of a pointing direction.

x-component of $\hat{x}$, which is the result of solving Equation (5) for the x-component and using the positive result when solving Equation (4) for the y- and z-components. The pointing direction of this unit vector always has a positive x-component relative to the fixed frame of the sternum. The glenoid fossa pointing direction angles, ϕ (*az*) and θ (*el*), can now be calculated as

$$\phi = \text{atan2}\left(\frac{y_\zeta}{x_\zeta}\right)$$
$$\theta = \text{asin}(z_\zeta), \tag{7}$$

where ϕ and θ are in degrees for this work.

The collected data were normalized to account for different body structures of the subjects, such as height, shoulder breadth and muscle mass. The normalization consisted of determining the distance from the sternum to the glenoid fossa when the subject's arm was pointed out to the side, directly along the x-axis (reference position for this work). All of the collected data were divided by this distance. A similar method was used in [18], with the only differences being the location of the reference point and the reference position. For that work, the reference point was the intersection of an axis passing medially/laterally through the center of the glenohumeral joint and an axis passing anteriorly/posteriorly through the sternum. The reference position was with the humerus pointing straight down to the side. The reason for the choice of the sternum as the reference point in this work is that it is a physically measurable point onto which a sensor can be directly placed. The reference position was chosen because it is located near the center of the humeral range of motion.

3.1. Comparison of individual subjects

The data collected for each of the individual subjects were compared to the remaining subjects of the same gender (a gender analysis is discussed in Subsection 3.2) to assess consistency during data collection and if it is appropriate to group all subjects together for analysis. To accomplish this, the x-y-z locations of the glenohumeral joint relative to the sternum (for simplicity, this will just be referred to as location throughout this section) were compared for each subject relative to the remaining subjects using a nearest neighbor search algorithm. This entailed using *for* loops in MATLAB to compare the distance from each location of a subject to all locations of the remaining subjects and choosing the minimum distance. This was acceptable because the number of data points were relatively small (60,000 and 102,000 for the first and second set of motion studies, respectively). More complicated search algorithms are employed to deal with large data sets, on the order of 1 million data points or greater [13]. The MATLAB function *knnsearch* (MATLAB's built-in nearest neighbor search method) was employed to verify the method used and the results were in agreement. In addition, the glenoid fossa pointing directions were compared for each of the nearest neighbor pairs to determine if the pairs were relevant. This was accomplished by taking the dot product of unit vectors along the glenoid fossa pointing directions.

Table 1
Average minimum nearest neighbor distance for individual subject glenoid fossa location and pointing direction dot products from the first set of motion studies

	Subject	1	2	3	4	5	6	7	8	9	10
Females	**Avg. Dist.**	0.104	0.015	0.013	0.019	0.019	0.012	0.020	0.021	0.025	0.020
	Dot Prod.	0.91	0.97	0.98	0.98	0.98	0.97	0.98	0.95	0.96	0.96
	Subject	11	12	13	14	15	16	17	18	19	20
Males	**Avg. Dist.**	0.012	0.015	0.015	0.030	0.016	0.018	0.011	0.014	0.013	0.015
	Dot Prod.	0.98	0.97	0.98	0.98	0.97	0.97	0.98	0.97	0.98	0.98

Table 2
Average minimum nearest neighbor distance for individual subject glenoid fossa location and pointing direction dot products from the second set of motion studies

	Subject	1	2	3	4	5	6					
Females	**Avg. Dist.**	0.013	0.022	0.021	0.022	0.019	0.023					
	Dot Prod.	0.97	0.97	0.96	0.92	0.98	0.97					
	Subject	7	8	9	10	11	12	13	14	15	16	17
Males	**Avg. Dist.**	0.029	0.012	0.009	0.014	0.013	0.016	0.042	0.012	0.053	0.005	0.008
	Dot Prod.	0.98	0.98	0.97	0.97	0.93	0.97	0.94	0.97	0.98	0.99	0.98

The average of the minimum distances between nearest neighbors (this will referred to as 'average distance' throughout this section for simplification) were computed and are reported in Tables 1 and 2 along with the glenoid fossa pointing direction dot product averages for the first and second set of motion studies, respectively. The average distance for female subjects was 0.027 ± 0.028 (mean $\pm$ st. dev.), and for male subjects it was 0.016 ± 0.005 for the first set of motion studies (as stated before, the data was normalized, so these values are a percentage of the nominal shoulder girdle width at the reference location). The average distance for subject 1 was more than 2 standard deviations (nearly 3) away from the average distance for the female subjects, so the data from this subject were not used for the remaining anlyses. Without subject 1, the average distance for female subjects was 0.018 ± 0.004. For the second set of motion studies, the average distance for female subjects was 0.020 ± 0.004 and for male subjects it was 0.019 ± 0.015. The average distance for subject 15 was more than 2 standard deviations away from the average distance for the male subjects, so the data from this subject were not used for the remaining anlyses. Without subject 15, the average distance for male subjects was 0.016 ± 0.011. The difference in average distance for these subjects may have resulted from improper placement of one or more sensors, shoulder impairment unbeknownst to the subject or abnormal shoulder structure. As for the pointing direction comparisons, the average value for the remaining female subjects in the first set of studies was 0.97 ± 0.01 with the lowest value being 0.95, which correspond to average angle values of 14.07° and 18.19°, respectively. The average value for the male subjects was 0.98 ± 0.01 with the lowest value being 0.97, which correspond to average angle values of 11.48° and 14.07°, respectively. For the second set of studies, the average value for the female subjects was 0.96 ± 0.02 with the lowest value being 0.92, corresponding to average angle values of 16.26° and 23.07°, respectively. The average value for the remaining male subjects was 0.97 ± 0.02 with the lowest value being 0.94, corresponding to average angle values of 14.07° and 19.95°, respectively. All of the reported values for the remaining subjects are within 2 standard deviations of the average values. These results indicate that the glenoid fossa pointing directions match well for the nearest neighbor pairs in the majority of subjects.

Previous studies [1, 3, 6, 7, 19] have shown that the range of motion for dominant and non-dominant shoulder movements is similar. The collected data for this work did not provide any relevant information regarding range of motion because the subjects were not specifically asked to move their arms to the extents of their range. The subjects were asked to move in a voluntary fashion, which means that they did not exert the force necessary to reach some of the extents of their range of motion. However, the data from the left-handed subjects were analyzed to determine if there

was a difference in the actual motion, not just the range of motion. Subjects 7 and 11 were the only left-handed subjects in the first set of motion studies, and there were none in the second set of studies. As can be seen from the results in Table 2, the motion of those subjects showed little variation compared to the other subjects, as both were within a standard deviation of the average value for all subjects of the same gender reported above. Although these results are from analysis of individual points within the workspace as opposed to the range of motion, the subjects who used their non-dominant shoulders showed little variation from those who used their dominant shoulder, just as the results reported by the authors from the range of motion analyses. However, no definitive conclusions can be drawn regarding dominant vs. non-dominant shoulder motion because of the limited data (only 2 subjects).

Aside from subject 1 in the first set of motion studies and subject 15 in the second set of motion studies, the data collected from the individual subjects matched well with the remaining subjects. Therefore, all data from the remaining subjects were grouped together by gender for the remaining analyses.

3.2. Comparison of female and male subjects

It has been shown that the shoulder range of motion for females is greater than that of males for certain rotations [1, 3, 5, 9]. As stated earlier, the collected data did not provide any relevant information regarding range of motion as the subjects were not specifically asked to move their arms to the extents of their range. However, the data were analyzed to determine if there was variation in the actual motion of the shoulder girdle between the female and male subjects along with the variation in range of motion. For this analysis, each glenohumeral joint location from the male subject pool was compared to all locations from the female subject pool using the nearest neighbor search algorithm. Again, the glenoid fossa pointing directions were compared for each of the nearest neighbor pairs to determine if the pairs were relevant. The same methods described in Subsection 3.1 were employed for this analysis. In the first set of studies, the average distance for the glenohumeral joint locations was 0.020 ± 0.017, and the average dot product for the glenoid fossa pointing directions of nearest neighbor pairs was 0.96 ± 0.05, which corresponds to an average angle value of 16.26°. In the second set of studies, the average distance for the glenohumeral joint locations was 0.019 ± 0.021, and the average dot product for the glenoid fossa pointing directions of nearest neighbor pairs was 0.96 ± 0.04, which corresponds to an average angle value of 16.26°. These values fall within one standard deviation of the averages shown in Subsection 3.1 for both the female and male subject pools within both sets of motion studies.

The results presented in this subsection indicate that there is no significant difference in the data collected from male vs. female subjects. Therefore, female and male subjects were grouped together for the remaining analyses.

3.3. Comparison of collected data from the two motion studies

The data collected from the two motion studies were compared to assess the consistency of the results obtained with two different types of motion capture equipment. For this analysis, each glenohumeral joint location from the second set of motion studies was compared to all of the locations from the first set of motion studies using the nearest neighbor search algorithm. Again, the glenoid fossa pointing directions were compared for each of the nearest neighbor pairs to determine if the pairs were relevant. The same methods discussed in Subsection 3.1 were employed to accomplish this analysis. The average distance for the glenohumeral joint locations was 0.016 ± 0.015, and the average dot product for the glenoid fossa pointing directions of nearest neighbor pairs was 0.97 ± 0.04, which corresponds to an average angle value of 14.07°. These values fall within one standard deviation of the averages shown in Subsections 3.1 and 3.2 for both the female and male subject pools within both sets of motion studies.

The results presented in this subsection indicate that the data collected in the first and second sets of motion studies are consistent. However, significant portions of data were lost during collection in the second set of studies because the equipment required that all sensors be in view of at least one of the cameras. Due to the nature of the studies being conducted, it was not possible to keep all sensors in the view of the cameras at all times, so there were gaps in the data collected. Therefore, the data were only used to demonstrate consistency with the first set of motion studies. The remaining analyses only use the data collected from the first set of studies.

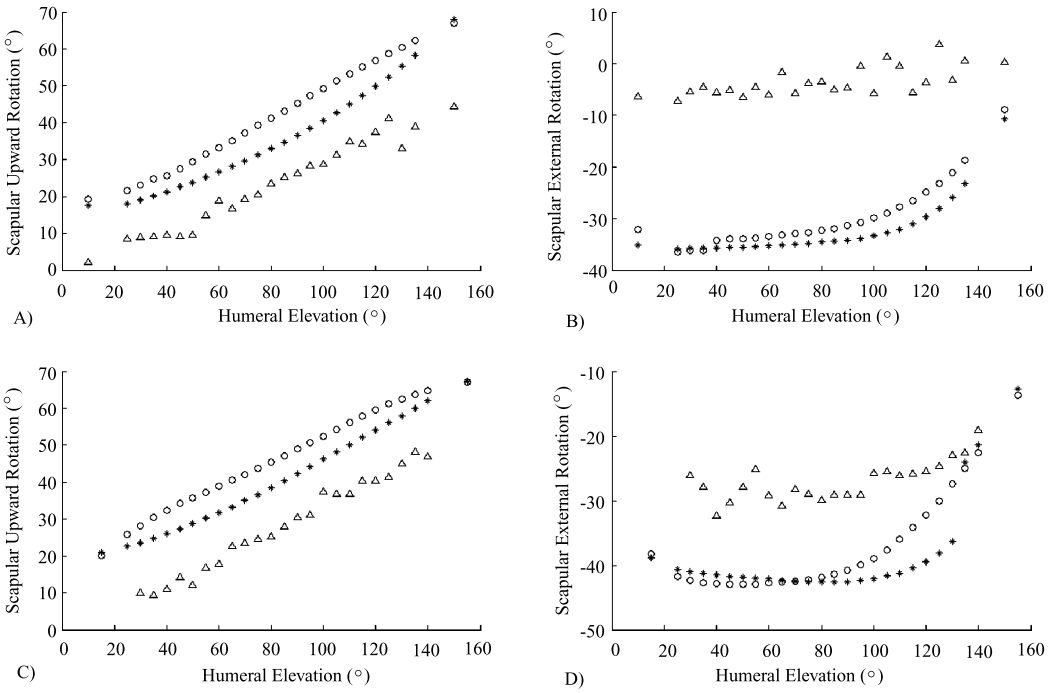

Fig. 4. A) Scapular upward rotation vs. humeral elevation in the scapular plane, B) scapular external rotation vs. humeral elevation in the scapular plane, C) scapular upward rotation vs. humeral elevation in the sagittal plane, D) scapular external rotation vs. humeral elevation in the sagittal plane. *: data from [22] during raising, o: data from [22] during lowering, △: data from this work.

4. Comparison of collected data to other work

The collected data were compared to reported results from other work to verify the motion capture method used here. This is important because the method used does not follow the protocols set in place by the ISB.

The first work selected for comparison was [22] because the method included fixing the pins directly into the scapula, to which the sensors were rigidly attached. This sensor placement ensures that the measurements are accurately tracking shoulder girdle motion (specifically scapular motion), as opposed to just moving with the skin. In addition, an electromagnetic tracking device (Polhemus 3Space Fastrak) was used for taking measurements, similar to the equipment used in the work reported here. These attributes made this an ideal candidate for comparison. Eight subjects were used in the motion studies (5 men and 3 women) with a mean age of 32.6 (27 to 37) years and an average body mass index of 25.2 $\frac{kg}{m^2}$ (19.1 to 35.2). All subjects were right-hand dominant, and the data for all subjects were grouped together for the analysis. The reported results included scapular measurements taken during humeral abduction in the scapular (plane rotated 40° about the positive z-axis from the frontal plane for this work[1]) and sagittal planes, for both raising and lowering the arm. The correct plane of elevation was maintained within ±5°. The measurements included scapular upward rotation (about the y-axis) and scapular external rotation (about the z-axis). The elbow was in full extension for all subjects during these motions, and it should be noted that the subjects were in a standing position during the studies. The reference position was with the arm straight down to the side, so the angles from the work presented here were adjusted to reflect this reference.

An open-source software package called Engauge Digitizer [11] was used to convert the graphical data from [22] into numbers for comparison purposes as it was not available in tabular format. Figure 4 shows the comparison, where the ∗ represents humeral raising and the ○ represents humeral lowering data points from [22] and the △ represents the data points from the work presented here. There is an obvious vertical

[1]The scapular plane has not been standardized; it can range anywhere from 30° to 45° forward of the frontal plane.

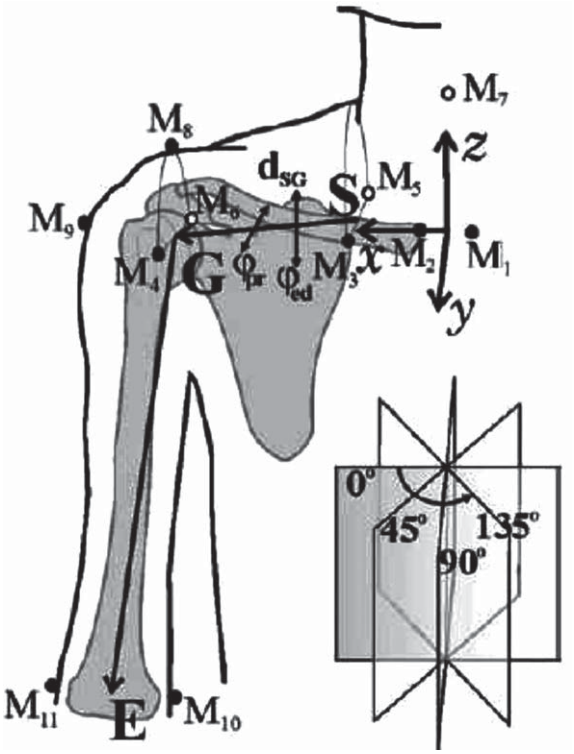

Fig. 5. Reference frame, sensor placement locations and four planes of elevation used in [18].

shift between the two sets of data, which is due to the difference in initial placement of the sensors for the reference position. For humeral elevation in the sagittal plane, no data were collected in this work at the elevation angles 15°, 25° and 155° presented in [22]. Pearson correlation coefficients were calculated using the MATLAB function *corrcoef* to determine how well the data sets matched; these values are listed in Table 3. The correlation coefficients for scapular upward rotation are high for both humeral motions. The values for scapular external rotation during humeral elevation in the sagittal plane were also fairly high. However, the values for scapular external rotation during humeral elevation in the scapular plane were lower. As can be seen graphically in Fig. 4, the data from [22] is linear until about 100°, at which point the scapular external rotation values start to increase exponentially. The results for the work presented here continue to follow a linear relationship, and do not exhibit the exponential relationship after 100°. This is likely due to the method used because, unlike [22], the sensors were not rigidly attached to the scapula. It is possible that the gross motion of the shoulder girdle (including the scapula, muscles, ligaments and tendons) do not follow the same motion as the scapula alone. Another possibility is that the data collected in the work here may have been affected by the compression shirt reaching its elastic limit, preventing it from continuing to follow the motion of the scapula. All of the p-values were less than 0.05 for the correlation coefficients, meaning they are statistically significant. Overall, the correlation between the data collected in this work and that reported in [22] is very good and shows that the data collected here exhibit similar trends.

The second work selected for comparison was [18] because results for shoulder heaving were presented. As stated earlier, this is an important aspect of the shoulder girdle motion, so this is a good candidate for comparison. An optical system with active infrared markers called Optotrak was used to record spatial positions of bony landmarks. The sensors were placed directly on the skin, but the means of attachment was not stated. The locations of the sensors are shown in Fig. 5 and labeled M1–M11. The locations of M1 and M2 are at the clavicle-sternum edge, M3 and M4 are in the anterior region of the shoulder girdle, M5

Table 3
Correlation coefficients for collected data compared to results reported in [22]

	Humeral Elevation			
	Scapular Plane		Sagittal Plane	
	Lowering	Raising	Lowering	Raising
Scapular Upward Rotation	0.9654	0.9863	0.9909	0.9923
Scapular External Rotation	0.5616	0.6223	0.7639	0.8484

$p < 0.05$ for all correlation coefficients, so the values are statistically significant.

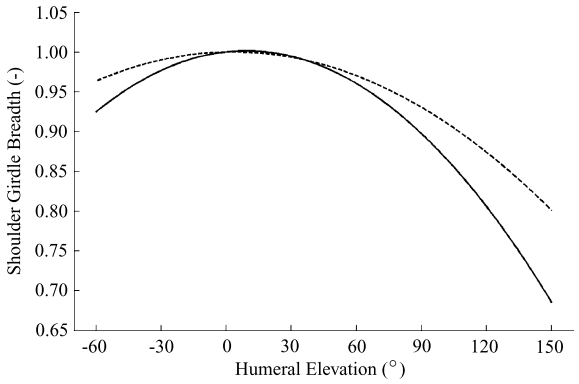

Fig. 6. Comparison of the shoulder girdle breadth vs. humeral elevation from [18] (solid) and this work (dashed).

and M6 are in the posterior region of the shoulder girdle, M7 is on the C7 vertebrae and M8 is on the clavicle acromion edge. Sensor M9 is located on the external edge of the humerus greater tubercle, M10 is on the medial epicondyle of the elbow and M11 is on the lateral epicondyle. The locations of sensors M3 and M5 are not clear, so estimates had to be made in order to move forward with the comparison, which will be discussed later. The subjects included 5 males (height of 181.0 ± 5.3 cm, weight of 78.2 ± 2.5 kg) and 5 females (height of 166.2 ± 4.9 cm, weight of 50.6 ± 1.7 kg) with an average age of 24.8 ± 1.4 years. All subjects were right-handed. The subjects were seated and leaning against the back of the chair, similar to the work presented here. The reference position was with the arm fully extended downward (in the negative z-direction) at the side of the body, and the reference point was at the intersection of a medial/lateral axis passing through the center of the glenohumeral joint and a posterior/anterior axis passing through the sternum. The subjects elevated their arms in four planes, including the frontal plane, scapular plane (plane rotated 45° about the positive z-axis from the frontal plane for this work), sagittal plane and a plane rotated 45° about the positive z-axis from the sagittal plane. There was no mention of angular variation from these planes during data collection. The subjects performed all motions dynamically with unilateral (one arm) and bilateral (both arms) humeral elevation, keeping the arm fully extended throughout the motion. Only the results from unilateral elevation are relevant for comparison here. All of the collected data from the different subjects and different planes of elevation were grouped together. To account for varying body structures, each subject's data were normalized by the distance from the point S (the center of markers M3 and M5) to the point G (the center of markers M4 and M6, representing the glenohumeral joint) in the reference position.

The following second order polynomial was reportedly fit to the data

$$GH = -1.6 \times 10^{-5}\varphi^2 + 3 \times 10^{-4}\varphi + 1, \quad (8)$$

where GH is the distance from S to G and the φ is the elevation angle of the humerus. The humerus is represented by a vector from G to E (the center of markers M10 and M11), and the elevation angle was calculated as the angle between the body's vertical axis and this vector.

Similar to the comparison with [22], the angular measurements had to be adjusted to reflect the different

reference position. A second order polynomial was fit to the data from this work to compare with the second order polynomial presented in [18], and Fig. 6 shows the curves, where the dashed curve represents the former and the solid curve represents the latter. The curves show a similar trend, but have a slightly different curvature. This difference may be due to the method used for attaching sensors, but is most likely attributed to the estimation of the sensor locations in [18]. The x-component of point S was estimated by measuring the graphic and was determined to be one-quarter of the distance from the center of the sternum to point G. The y- and z-components were calculated using data collected in the work presented here by dividing the y- and z-axis distances to the glenohumeral joint from the sternum by the total glenohumeral distance near the reference position (within a 10° cone). This was completed for all subjects, and the average values were calculated to be 0.4376 and 0.0954 for y- and z-components, respectively. These values were used as an offset to compare results from the same reference point. In addition, the glenohumeral joint distance at the reference point was used to normalize the remaining distances, as was done in [18]. The Pearson correlation coefficient for the curves is 0.9797 with a p-value less than 0.05. The lack of information about sensor location makes this comparison difficult, but the intent was to show that there is a similar trend between the results. The high correlation coefficient value indicates that this is the case.

The final work chosen for comparison was [4] because the location of the glenohumeral joint was measured along with scapular rotation during humeral elevation, which most closely reflects the goals of this work. The measurement methods included using a liquid-filled goniometer to determine the humeral elevation and an electromagnetic tracking device, IsotrakII. The transmitter for the IsotrakII system was mounted on a Locator, which has legs specially designed to make repeatable measurements of three bony landmarks, namely the posterior angle of the acromion, the root of the scapular spine and the inferior angle. A receiver was mounted vertically on the sternum, and this was the reference location. The tests were completed with five subjects, but no information was given on age, gender, height or weight. The reference position was with the humerus pointing straight down at the subject's side. Measurements were taken at 10° increments from 10° to 90° in the frontal plane, and the arm was only allowed to vary within ±5° of this plane. The measurements included scapular upward rotation, scapular external rotation and x-, y- and z-displacements (in mm) of the glenohumeral joint. It should be noted that the measurements were taken during static poses and with the elbow flexed 90°. It was not stated if the subjects were seated or standing during testing. All of the data collected from the subjects were grouped together.

Engauge Digitizer was used to convert the graphical data into numbers for comparison. In order to compare the glenohumeral joint locations, the normalized values from the work presented here had to be converted to mm, which was accomplished by multiplying the normalized values by the average distance from the sternum to the glenohumeral joint for all subjects near the reference position (within a 10° cone). Once again, the angular measurements were adjusted to account for the different reference position. Figure 7 shows a graphical comparison, where the data reported by [4] are shown with an $*$ and the work presented here is shown with a $\triangle$. The scapular upward rotation curves for the two data sets match up well graphically, and this is supported by a Pearson correlation coefficient value of 0.9902. The scapular external rotation curves have more variation, but still follow a similar trend, supported by a high correlation coefficient of 0.9612. The curves representing the x-, y- and z-displacements of the glenohumeral joint match well for the first 70° of humeral elevation, at which point the curves start to deviate. These curves also have high correlation coefficients of 0.8935, 0.9205 and 0.9461 for x-, y- and z-displacements of the glenohumeral joint, respectively. The deviations between the curves are likely due to the difference in methods used between the two studies. As stated earlier, the sensors for the work presented in [4] were attached directly to the skin, whereas the sensors for the work presented here were attached to a compression shirt. The skin moves in the same direction as the scapula, but they do not move in a one-to-one relationship because the skin can stretch and slide over the scapula. The compression shirt used for the work here suffers the same shortcoming. The data collected in both studies may have been affected by elastic limits of the skin or compression shirt, preventing the sensors from accurately following the motion of the scapula and one another. However, the comparison of the results indicate that the the data from both studies are following a similar trend. This comparison was significant because it shows that the data collection method used for this work produced a similar trend to

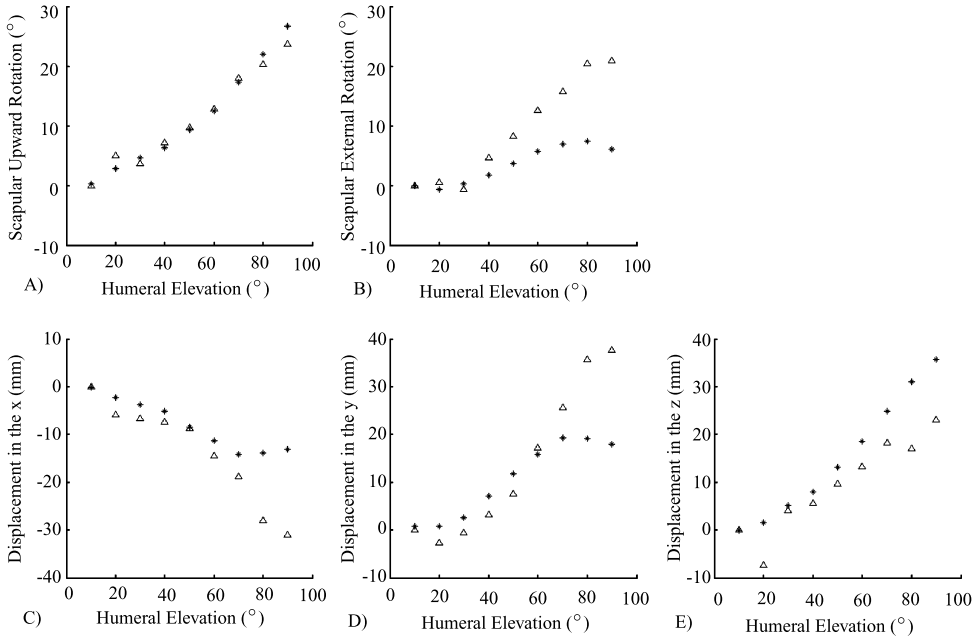

Fig. 7. A) Scapular upward rotation vs. humeral elevation in the frontal plane, B) scapular external rotation vs. humeral elevation in the frontal plane, C) displacement in the x vs. humeral elevation in the frontal plane, D) displacement in the y vs. humeral elevation in the frontal plane and E) displacement in the z vs. humeral elevation in the frontal plane. *: data from [4], Δ: data from this work.

an established method for measuring scapular rotation and displacement.

The strong correlation between the data collected here and the results against which they were compared indicates that the methods used provided results that are in agreement with established methods for data collection. This was important to provide validation to the results that will be presented in the following sections.

5. Surface fits of the collected data

Having established that the data collected is consistent with prior literature. the motion of the human shoulder girdle relative to the humeral pointing direction for voluntary motion was quantified, which is one of the major contributions of this work. As stated earlier, the motion of the shoulder girdle is coupled to humeral pointing. Therefore, the most relevant way to display the data collected in this work is to show the parameters describing shoulder girdle motion relative to humeral pointing direction angles. The parameters describing shoulder girdle motion include the two pointing angles, ϕ and θ, for the glenoid fossa pointing direction and the x-y-z locations of the shoulder girdle. Polynomial least square surfaces were fit to the collected data to represent the data from all subjects. The goal was to balance the smoothness, by minimizing the degree of the polynomial, and the goodness of fit, by improving the coefficient of determination (also known as the r-squared value, which is the square of the Pearson correlation coefficient). High order polynomials generally have sharp peaks within the data

Table 4
Coefficients of determination (R-squared values) for different polynomial degree surface fits of the shoulder girdle motion parameters

	Degree			
	2^{nd}	3^{rd}	4^{th}	5^{th}
ϕ	0.8939	0.9055 (0.013)	0.9085 (0.003)	
θ	0.8227	0.8335 (0.013)	0.8347 (0.001)	
x	0.7114	7254 (0.019)	0.7454 (0.027)	0.7495 (0.005)
y	0.7807	0.7900 (0.012)	0.7946 (0.006)	
z	0.5217	0.5447 (0.042)	0.5459 (0.002)	

()-values in parentheses show improvement over the previous polynomial degree.

range used for the fit and large variations outside of it, but low order polynomials do not capture the intricate variations within the data range used for the fit. Therefore, it is a matter of finding a good balance between the two. The MATLAB function *fit* was employed to calculate the surface fit coefficients and the coefficient of determination. In order to find the most appropriate fit, surface fits were created for the polynomial degrees shown in Table 4, and the coefficients of determination were calculated for each. The coefficients of determination were then compared, and a polynomial degree was selected if the next degree showed less than 1% improvement (improvement over the previous degree is shown in parentheses). The x location was the only parameter that required higher than a 3^{rd} degree polynomial (4^{th} degree). Some of the r-squared values may appear to be low (z location particularly), but they are the squares of the Pearson correlation coefficient. These values correspond to correlation coefficients of 0.9516, 0.9130, 0.8634, 0.8888 and 0.7380 for ϕ, θ, x, y and z, respectively, which all imply good correlation. The relatively low value for z is most likely due to the natural tendencies of the subjects. For example, some of the subjects may have had a tendency to shrug their shoulders more than others during the motion studies due to musculature or tension caused by anxiety or other factors. Shoulder shrugging would also affect the x and y parameters, but not to the same degree.

The following are the surface fit equations for the different parameters

$$\begin{aligned}
\phi =& -17 + 0.043\rho + 0.53\psi + 6.2e^{-4}\rho^2 + 6.4e^{-4}\rho\psi \\
& -7.9e^{-4}\psi^2 + 2.8e^{-6}\rho^3 - 3.8e^{-5}\rho^2\psi \\
& -6.0e^{-6}\rho\psi^2 + 8.5e^{-6}\psi^3 \\
\theta =& -24 + 0.32\rho - 0.036\psi - 4.7e^{-4}\rho^2 - 1.8e^{-4}\rho\psi \\
& -3.8e^{-4}\psi^2 - 1.9e^{-6}\rho^3 + 7.3e^{-6}\rho^2\psi \\
& +1.2e^{-5}\rho\psi^2 - 8.3e^{-6}\psi^3 \\
x =& \ 0.70 + 1.9e^{-3}\rho + 4.3e^{-3}\psi - 1.2e^{-5}\rho^2 \\
& +1.8e^{-5}\rho\psi - 5.2e^{-5}\psi^2 - 9.7e^{-8}\rho^3 \\
& -2.3e^{-7}\rho^2\psi - 2.1e^{-7}\rho\psi^2 - 8.6e^{-8}\psi^3 \\
& -2.9e^{-10}\rho^4 + 2.8e^{-10}\rho^3\psi + 5.7e^{-9}\rho^2\psi^2 \\
& +4.8e^{-10}\rho\psi^3 + 1.8e^{-9}\psi^4 \\
y =& -0.70 + 1.2e^{-3}\rho + 4.3e^{-3}\psi + 6.2e^{-6}\rho^2 \\
& +1.5e^{-5}\rho\psi - 1.4e^{-5}\psi^2 - 6.5e^{-8}\rho^3 \\
& -2.6e^{-7}\rho^2\psi - 7.5e^{-8}\rho\psi^2 + 7.0e^{-8}\psi^3 \\
z =& -7.7e^{-3} - 2.3e^{-3}\rho + 7.7e^{-5}\psi - 4.7e^{-6}\rho^2 \\
& -7.8e^{-6}\rho\psi - 7.3e^{-6}\psi^2 + 6.2e^{-8}\rho^3 \\
& +4.5e^{-8}\rho^2\psi + 5.9e^{-8}\rho\psi^2 + 1.6e^{-7}\psi^3, \quad (9)
\end{aligned}$$

where ϕ and θ have units of degrees and x, y and z are unitless because they represent the normalized location of the glenohumeral joint relative to the sternum. These equations completely quantify the gross shoulder girdle motion relative to humeral pointing, allowing for determination of position and orientation of the glenohumeral joint.

6. Conclusion

This paper has presented a complete characterization of human shoulder girdle motion relative to humeral pointing. Motion studies were conducted for collecting data on the motion of the shoulder girdle relative to the motion of the humerus during voluntary motion. A thorough analysis was completed on the collected data to show that it was reasonable to group the subjects together for the characterization of the motion. A second set of motion studies was conducted and a comparison of the collected data showed consistency with the first set of studies. This helped to alleviate concerns over the type of equipment used.

The comparison of the collected data to other work showed strong correlation, indicating that the results exhibit a similar trend to published work. This was significant because the method used did not strictly follow the protocol put forth by the ISB.

The collected data were used to create surface fit equations that completely describe the motion of the human shoulder girdle relative to the humeral pointing direction. These equations may be used as a reference for future shoulder motion studies. They may also provide equations of motion for a humanoid or prosthetic shoulder mechanism to closely replicates human shoulder motion.

The next challenge will be to create a 2-DOF humanoid shoulder girdle mechanism using the collected data and equations presented here. The mechanism would then have the same coupling between position and orientation seen in the human shoulder girdle. This will enable the replication of the complex human shoulder girdle motion with a relatively simple robotic system.

Acknowledgment

The authors would like to thank the subjects who volunteered to participate in these motion studies for their time and the use of their shoulders.

References

[1] E. Allander, et al. Normal range of joint movements in shoulder, hip, wrist and thumb with special reference to side: A comparison between two populations, *International Journal of Epidemiology* **3**(3) (1974), 253-261.

[2] Ascension Technology Corporation, PO Box 527, Burlington, VT 05402 USA. *Flock of Birds Real Time Motion Tracking,* 2000.

[3] C. Barnes, S. Van Steyn and R. Fischer, The effects of age, sex, and shoulder dominance on range of motion of the shoulder, *Journal of Shoulder and Elbow Surgery* **10**(3) (2001), 242-246.

[4] N. Barnett, R. Duncan and G. Johnson, The measurement of three dimensional scapulohumeral kinematics - a study of reliability, *Clinical Biomechanics* **14**(4) (1999), 287-290.

[5] C. Bonci, F. Hensal and J. Torg, A preliminary study on the measurement of static and dynamic motion at the glenohumeral joint, *The American Journal of Sports Medicine* **14**(1) (1986), 12-17.

[6] D. Boone and S. Azen, Normal range of motion of joints in male subjects, *Journal of Bone and Joint Surgery* **61**(5) (1979), 756.

[7] G. Clarke, et al. Preliminary studies in measuring range of motion in normal and painful stiff shoulders, *Rheumatology and Rehabilitation* **14**(1) (1975), 39-46.

[8] S. Dorinson and M. Wagner, An exact technic for clinically measuring and recording joint motion, *Archives of Physical Medicine and Rehabilitation* **29**(8) (1948), 468-475.

[9] N. Doriot and X. Wang, Effects of age and gender on maximum voluntary range of motion of the upper body joints, *Ergonomics* **49**(3) (2006), 269-281.

[10] Z. Dvir and N. Berme, The shoulder complex in elevation of the arm: A mechanism approach, *Journal of Biomechanics* **11**(5) (1978), 219-225.

[11] Engauge digitizer– digitizing software.

[12] A. Engin and S. Tumer, Three-dimensional kinematicmodelling of the human shoulder complex–part i: Physical model and determination of joint sinus cones, *Journal of Biomechanical Engineering* **111**(2) (1989), 107-112.

[13] J. Friedman, J. Bentley and R. Finkel, An algorithm for finding best matches in logarithmic expected time, *ACM Transactions on Mathematical Software (TOMS)* **3**(3) (1977), 209-226.

[14] S. Hoppenfeld, Physical Examination of the Spine and Extremeties. Appleton-Century-Crofts, Norwalk, CT 1976.

[15] V. Inman, J. Saunders and L. Abbott, Observations on the function of the shoulder joint, *Journal of Bone Joint Surgery* **26**(1) (1944), 1-30.

[16] I. Kapandji, The Physiology of the Joints. Churchill Livingstone, New York, NY, 1985.

[17] F. Kendall and E. McCreary, *Muscle Testing and Function*. Williams and Wilkins, Baltimor, MD, 1983.

[18] N. Klopčar and J. Lenarčič, Bilateral and unilateral shoulder girdle kinematics during humeral elevation, *Clinical Biomechanics* **21**(SUPPL. 1) (2006), S20-S26.

[19] M. Kronberg, L. Brostrom and V. Soderlund, Retroversion of the humeral head in the normal shoulder and its relationship to the normal range of motion, *Clinical Orthopaedics and Related Research* **253** (1990), 113-117.

[20] J. Lenarčič and M. Stanišič, A humanoid shoulder complex and the humeral pointing kinematics, *IEEE Journal of Robotics and Automation* **19**(3) (2003), 499-506.

[21] J. Lenarčič, M. Stanišič and V. Parenti-Castelli, A 4-dof parallel mechanism simulating the movement of the human sternum-clavicle-scapula complex. *Advances in Robot Kinematics*, (2003), pp. 325-332, 2000.

[22] P. McClure, et al. Direct 3-dimensional measurement of the scapula kinematics during dynamic movements *in vivo*, *Journal of Shoulder and Elbow Surgery* **10**(3) (2001), 269-277.

[23] E. McFarland, *Examination of the Shoulder: The Complete Guide*. Thieme Medical Publishers, Inc., New York, NY, 2006.

[24] C. Meskers, et al. 3d shoulder position measurements using a six-degree-of-freedom electromagnetic device, *Clinical Biomechanics* **13**(4–5) (1998), 280-292.

[25] C. Oatis, *Kinesiology: The mechanics and pathomechanics of human motion*. Lippincot, Williams and Wilkins, Philadelphia, PA, 2004.

[26] M. Stanišič and O. Duta, Symmetrically actuated double pointing systems: The basis of singularity-free robot wrists, *IEEE Transactions on Robotics and Automation* **6**(5) (1990), 562-569.

[27] M. Stokdijk, J. Nagels and P. Rozing, The glenohumeral joint rotation centre *in vivo*, *Journal of Biomechanics* **33**(12) (2000), 1629-1636.

[28] H. Veeger, The position of the rotation center of the glenohumeral joint, *Journal of Biomechanics* **33**(12) (2000) 1711-1715.

[29] G. Wu, et al. Isb recommendation on definitions of joint coordinate systems of various joints for the reporting of human joint motion–part II: Shoulder, elbow, wrist and hand, *Journal of Biomechanics* **38**(5) (2005), 981-992.

[30] V. Zatsiorsky, Kinematics of Human Motion. Human Kinematics, Champaign, IL, 1998.